PMU-based system state estimation for multigrounded distribution systems

P. M. De Oliveira-De Jesus, *Senior Member, IEEE*, N. A. Rodriguez, D. F. Celeita, *Senior Member, IEEE*, G. A. Ramos, *Senior Member, IEEE*

***Abstract*—Linear network modeling and phasor measurement units (PMUs) simplify the traditional system state estimation (SSE) problem. The existing multiphase SSE-PMU-based models are linear including earthing resistances as a fixed and invariable parameter. However, earthing resistances strongly depend on moisture and temperature changes over time. Thus, under unbalanced operation time-varying Neutral-Earth Voltages (NEV) could be higher than admisible touch and step voltages in urban areas. Earthing resistances can be now monitored using specialized meters and therefore duly incorporated as measured and state variables in a multigrounded SSE problem. Thus, the SSE problem becomes non-linear and the standard linear solution approach is no longer suitable. This fact has been overlooked in the literature. To fulfill the research gap, a new multi-grounded SSE-PMU-based formulation is presented. As a key contribution, the normal-equation structure used in linear SSE approaches was extended to a non-linear one in order to allow the estimation of grounding resistances, neutral-to-earth voltages, and neutral currents. The proposal was applied in a 2-bus example for illustration purposes and successfully applied and compared with existing methods under large-scale conditions.**

***Index Terms*—Distribution system, state estimation, Grounding, earthing resistance measurement, phasor measurement units**

I. Introduction

System state estimation is the cornerstone of future power systems [1]. State estimators can provide an appropriate mathematical framework for validating the field measurements against the model of the components of the transmission and distribution system.

The current trend shows that traditional system state estimators (SSE) based on power measurements could be progressively substituted by ones on which current and voltage variables are synchronized using phasor measurement units (PMU). The solution of the weighted least square (WLS) state estimation problem in the three-phase domain is straightforward since the resulting mathematical model is linear [2]. Given a set of m measurements ($\widehat{\boldsymbol{z}}$) and a weighting matrix ($\mathbf{W}$), to find out the vector of n_v voltages ($\boldsymbol{v}$) does not require any iterative process since the Jacobian ($\mathbf{H}$) and the gain matrix ($\mathbb{G}$=$\mathbf{H^T W H}$) are linear [2], [3]: $\boldsymbol{v} = \mathbb{G}^{-1}\mathbf{H^T W}\widehat{\boldsymbol{z}}, m \geq n_v$.

Manuscript received November 8, 2019

P. M. De Oliveira-De Jesus (Email: pm.deoliveiradejes@uniandes.edu.co), D. F. Celeita (Email: df.celeita10@uniandes.edu.co), N. A. Rodriguez (Email: na.rodrigues10@uniandes.edu.co) and G. A. Ramos (Email: gramos@uniandes.edu.co) are with the Department of Electrical and Electronic Engineering, School of Engineering, Universidad de los Andes, Bogotá, Colombia.

Digital Object Identifier

There are important differences between SSE methods applied at transmission and distribution level. SSE methods in transmission are based on the traditional three-phase and positive sequence network model where variations on neutrals and grounding parameters are neglected since unbalanced currents are low. Conversely, next generation distribution systems are inherently unbalanced and must be modeled as multiphase and multigrounded systems [4], [5] where earthing resistances (r_k) as a function of soil resistivity are strongly dependent on temperature (T) and moisture (M) [6]. As a result, time varying dangerous neutral-earth voltages (NEV: $v_k^n(T,M)$=$r_k(T,M)i_k^{ng}(T,M)$) can appear jeopardizing system safety, e.g. NEVs higher than tolerable touch voltages in urban areas [6]. Earthing resistances can be now monitored on the spot using different conventional measurement technologies such as [8]. For instance, EPRI visualizes the widespread monitoring of earthing resistances in the near future [9]. Therefore, earthing resistances are time-varying magnitudes suitable to be incorporated as state variables and measurements of the SSE problem. This fact has been completely overlooked in all existing SSE proposals.

The literature on SSE models is vast and comprehensive reviews can be found in [10]–[12]. Table I divides relevant literature in two major groups considering whether the SSE formulations are non-linear –by solving $\mathbf{s}$=$\mathbf{vi}^*$ iteratively– or linear –by solving $\mathbf{i}$=$\mathbf{Yv}$ with direct solutions–. Both groups can use positive sequence, three-phase or 4-wire/multiphase network models to pose the optimization problem. Three-phase linear and non-linear SSE approaches are included in the first and third column of the table, respectively. Positive sequence approaches are not included in the table. Recently, a method based on 4-wire network models was introduced by [13] as shown in the third column of Table I. However, this model does not consider earthing resistances as state variables. The inclusion of earthing resistances in the SSE are crucial to improve system observability associated with the behavior of neutral voltages during steady-state and fault conditions [10].

To fulfill the research gap, this paper presents a new WLS-PMU-SSE procedure based on a multigrounded distribution network model. As a key contribution, we redefine the structure of the normal-equation in order to include sets of earthing resistances ($\boldsymbol{r}$) as state and measured variables:

$$[\boldsymbol{v},\boldsymbol{r}]^{\nu+1} = [\boldsymbol{v},\boldsymbol{r}]^{\nu} + \mathbb{G}(\boldsymbol{v},\boldsymbol{r})^{-1}\mathbf{H}(\boldsymbol{v},\boldsymbol{r})^{\mathbf{T}}\mathbf{W}[\widehat{\boldsymbol{z}} - \boldsymbol{h}(\boldsymbol{v},\boldsymbol{r})]$$

In this case, the gain $\mathbb{G}$ and the Jacobian matrix $\mathbf{H}(\mathbf{v},\mathbf{r})$ of $\boldsymbol{h}(\boldsymbol{v},\boldsymbol{r})$ become non-linear allowing the estimation of earthing resistances as well as three-phase and neutral voltages. There-

TABLE I
SUMMARY OF EXISTING SSE PROCEDURES

Reference	Linear		Non-Linear	
	3p[1]	4w[2]	3p[1]	4w[2]
Mak, 2011 [17]	○			
Heydt, 2013 [18]	○			
Pau, 2013 [19]	○			
Meliopoulos, 2014 [2]	○			
Kong, 2018 [20]	○			
Chen, 2019 [21]	○			
Liu, 2019 [13]		○		
Wu, 1990 [22]			○	
Roytelman, 1993 [23]			○	
Baran, 1995 [24]			○	
Lu, 1995 [25]			○	
Wu, 2012 [26]			○	
Gol, 2014 [27]			○	
De Oliveira, 2015 [28]			○	
Dzafic, 2017 [29]			○	
Zhang, 2019 [30]			○	
Pokhrel, 2019 [31]			○	
Chen, 2019 [32]			○	
This paper				•

[1] 3p=Three-phase network model
[2] 4w=4 wire/multiphase network model

fore, this proposal is enclosed in the fourth column of Table I as a new non-linear SSE method based on 4-wire/multiphase network models. The extended normal equation can be solved via Newton with any existing factorization methodology. The contribution of the paper is circumscribed to extend existing linear SSE models [2] in order to estimate new elements such as neutral-to-earth voltages, earthing resistances and neutral and earth currents. Despite we solve the normal equation under large scale conditions, finding the best factorization method for the extended gain matrix is out of the scope of the paper and matter of future research. The proposal was illustrated using a simple two-bus example and under large-scale conditions. Observability analysis, bad data detection and identification are also discussed from the results. A comparison study with the linear 3-phase SSE model [2] and 4-wire [13] SSE is also provided.

The paper is organized as follows. Section II is devoted to describing the network model used in this proposal. Section III presents the proposed formulation. A test case is defined in section IV. The results are discussed in Section V. Conclusions are drawn in Section VI.

The notation is defined as follows. Matrices are denoted in boldface capital letters. Vectors are expressed in boldface italicized lower-case letters. The scalars are represented as lower-case italicized letters. Complex numbers are overlined letters. The capital letter $\mathbf{T}$ designates the transpose of a matrix or a vector. Lower-case letter i has different meanings depending on the context. Italicized letter i refers to a bus number when it is used as a subscript. Italicized i letter also refers to an injected current variable expressed in amperes. Non-italicized letter i denotes the complex number operator: $\overline{a}$=a^r+$\mathbf{i}a^i$ where a^r is the real part of $\overline{a}$ and a^i is the imaginary part of $\overline{a}$.

II. THE MULTIGROUNDED NETWORK MODEL

In this section, the multigrounded network model defined in [4] is described in detail. The description of the multigrounded network model structure is absolutely necessary to formulate our proposal in Section III.

Consider the meshed network depicted in Fig. 1. The system has n_b *monitored buses*, i.e. buses associated with a load or a distributed generator. The distribution line between a bus i and a bus k is modeled as a 4-wire network through series and shunt primitive admittances ($\widetilde{\mathbf{Y}}_{\mathbf{ik}}$=$\widetilde{\mathbf{G}}_{\mathbf{ik}}$+$\widetilde{\mathbf{B}}_{\mathbf{ik}}$i and $\widetilde{\mathbf{Y}}^{\mathbf{sh}}_{\mathbf{ik}}$=$\widetilde{\mathbf{B}}^{\mathbf{sh}}_{\mathbf{ik}}$i). Details of how to determine primitive admittances of untransposed 4-wire distribution systems can be reviewed in [15]. The 4-wire model was chosen in virtue of its simplicity. However, the model can be easily extended to several circuits in the same right of way of the distribution line using appropriate Kron's reductions. The system admittance matrix $\mathbf{Y}$ is structured according to the network topology. The relationship between all nodal injected currents and voltages is linear: $\boldsymbol{i}$=$\mathbf{Y}\boldsymbol{v}$=$\mathbf{G}\boldsymbol{v}$ + i$\mathbf{B}\boldsymbol{v}$ where $\mathbf{G}$ and $\mathbf{B}$ are the conductance and susceptance system matrices, respectively. The elements of the admittance matrix $\mathbf{Y}$ are: $g^{pq}_{ik} \in \mathbf{G_{ik}}$ and $b^{pq}_{ik} \in \mathbf{B_{ik}}$

The set of all voltages of the system is defined in volts as $\boldsymbol{v}$=$[\boldsymbol{v_1}, \ldots, \boldsymbol{v_k}, \ldots, \boldsymbol{v_{n_b}}]$ where $\boldsymbol{v_k}$=$[\overline{v}^a_k, \overline{v}^b_k, \overline{v}^c_k, \overline{v}^n_k]^{\mathbf{T}}$ for phases a, b, c and neutral n. Nodal voltages can be expressed in rectangular or polar coordinates and referenced concerning an external bus voltage $\boldsymbol{v_0}$. Thus, the voltage at bus k is denoted $\boldsymbol{v_k}$=$[v^a_k e^{\theta^a_k \mathbf{i}}, v^b_k e^{\theta^b_k \mathbf{i}}, v^c_k e^{\theta^c_k \mathbf{i}}, v^n_k e^{\theta^n_k \mathbf{i}}]^{\mathbf{T}}$ where v^a_k, v^b_k and v^c_k, are the magnitudes of the line to ground voltages at each phase. Each angle θ^q_k indicates the voltage angle position synchronized via PMUs with an external angle reference.

The set of all injected currents of the system is defined in amperes as $\boldsymbol{i}$=$[\boldsymbol{i_1}, \ldots, \boldsymbol{i_k}, \ldots, \boldsymbol{i_{n_b}}]$ where $\boldsymbol{i_k} = [\overline{i}^a_k, \overline{i}^b_k, \overline{i}^c_k, \overline{i}^n_k]^{\mathbf{T}}$ for phases a, b, c and neutral n. At each bus k, neutral is earthed through an earthing resistance r_k in ohms. Thus, the injected neutral currents should accomplish:

$$\overline{i}^a_k + \overline{i}^b_k + \overline{i}^c_k + \overline{i}^n_k + \overline{i}^g_k = 0 \tag{1}$$

where the injected current at ground $\overline{i}^g_k$ at bus k coincides with the current flowing through the resistance r_k from neutral terminal to ground terminal, that is:

$$\overline{i}^g_k = \overline{v}^n_k / r_k = -\overline{i}^a_k - \overline{i}^b_k - \overline{i}^c_k - \overline{i}^n_k \tag{2}$$

Equations 1 and 2 must be also defined in their real an imaginary parts at each bus k=1,...,n_b:

$$i^{n,r}_k = -i^{a,r}_k - i^{b,r}_k - i^{c,r}_k - v^{n,r}_k / r_k \tag{3}$$
$$i^{n,i}_k = -i^{a,i}_k - i^{b,i}_k - i^{c,i}_k - v^{n,i}_k / r_k \tag{4}$$
$$i^{g,r}_k = -i^{a,r}_k - i^{b,r}_k - i^{c,r}_k - i^{n,r}_k = v^{n,r}_k / r_k \tag{5}$$
$$i^{g,i}_k = -i^{a,i}_k - i^{b,i}_k - i^{c,i}_k - i^{n,i}_k = v^{n,i}_k / r_k \tag{6}$$

The system admittance matrix does not include information of neutral grounding. Thus, general equation $\boldsymbol{i}$=$\mathbf{G}\boldsymbol{v}$+i$\mathbf{B}\boldsymbol{v}$ must be modified to include equations 3-6 and consider the ground path [4].

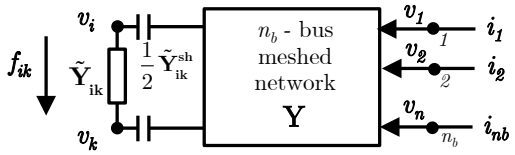

Fig. 1. The 4-wire network model.

The modified system admittance matrix (denoted *) including neutral earthing through a resistance is expressed in rectangular coordinates as:

$$\begin{bmatrix} \boldsymbol{i^r} \\ \boldsymbol{i^i} \end{bmatrix} = \begin{bmatrix} \mathbf{G}^* & -\mathbf{B}^* \\ \mathbf{B}^* & \mathbf{G}^* \end{bmatrix} \cdot \begin{bmatrix} \boldsymbol{v^r} \\ \boldsymbol{v^i} \end{bmatrix} \tag{7}$$

where,

$$\mathbf{G}^* = \begin{bmatrix} \mathbf{G^*_{11}} & \mathbf{G^*_{1i}} & \mathbf{G^*_{1k}} & \mathbf{G^*_{1n_b}} \\ \mathbf{G^*_{i1}} & \mathbf{G^*_{ii}} & \mathbf{G^*_{ik}} & \mathbf{G^*_{in_b}} \\ \mathbf{G^*_{k1}} & \mathbf{G^*_{ki}} & \mathbf{G^*_{kk}} & \mathbf{G^*_{kn_b}} \\ \mathbf{G^*_{n_b1}} & \mathbf{G^*_{n_bi}} & \mathbf{G^*_{n_bk}} & \mathbf{G^*_{n_bn_b}} \end{bmatrix} \tag{8}$$

$$\mathbf{B}^* = \begin{bmatrix} \mathbf{B^*_{11}} & \mathbf{B^*_{1i}} & \mathbf{B^*_{1k}} & \mathbf{B^*_{1n_b}} \\ \mathbf{B^*_{i1}} & \mathbf{B^*_{ii}} & \mathbf{B^*_{ik}} & \mathbf{B^*_{in_b}} \\ \mathbf{B^*_{k1}} & \mathbf{B^*_{ki}} & \mathbf{B^*_{kk}} & \mathbf{B^*_{kn_b}} \\ \mathbf{B^*_{n_b1}} & \mathbf{B^*_{n_bi}} & \mathbf{B^*_{n_bk}} & \mathbf{B^*_{n_bn_b}} \end{bmatrix} \tag{9}$$

The elements of $\mathbf{G}^*$ and $\mathbf{B}^*$ are given by

$$\mathbf{G^*_{ik}} = \begin{bmatrix} g^{aa}_{ik} & g^{ab}_{ik} & g^{ac}_{ik} & g^{an}_{ik} \\ g^{ba}_{ik} & g^{bb}_{ik} & g^{bc}_{ik} & g^{bn}_{ik} \\ g^{ca}_{ik} & g^{cb}_{ik} & g^{cc}_{ik} & g^{cn}_{ik} \\ g^{na}_{ik} & g^{nb}_{ik} & g^{nc}_{ik} & g^{nn}_{ik} \\ g^{na'}_{ik} & g^{nb'}_{ik} & g^{nc'}_{ik} & g^{nn'}_{ik} \end{bmatrix} \quad i \neq k \tag{10}$$

where $g^{na'}_{ik}$=$-g^{aa}_{ik} - g^{ba}_{ik} - g^{ca}_{ik}$, $g^{nb'}_{ik}$=$-g^{ab}_{ik} - g^{bb}_{ik} - g^{cb}_{ik}$, $g^{nc'}_{ik}$=$-g^{ac}_{ik} - g^{bc}_{ik} - g^{cc}_{ik}$ and $g^{nn'}_{ik}$=$-g^{an}_{ik} - g^{bn}_{ik} - g^{cn}_{ik}$

$$\mathbf{B^*_{ik}} = \begin{bmatrix} b^{aa}_{ik} & b^{ab}_{ik} & b^{ac}_{ik} & b^{an}_{ik} \\ b^{ba}_{ik} & b^{bb}_{ik} & b^{bc}_{ik} & b^{bn}_{ik} \\ b^{ca}_{ik} & b^{cb}_{ik} & b^{cc}_{ik} & b^{cn}_{ik} \\ b^{na}_{ik} & b^{nb}_{ik} & b^{nc}_{ik} & b^{nn}_{ik} \\ b^{na'}_{ik} & b^{nb'}_{ik} & b^{nc'}_{ik} & b^{nn'}_{ik} \end{bmatrix} \forall i,k \tag{11}$$

where $b^{na'}_{ik}$=$-b^{aa}_{ik} - b^{ba}_{ik} - b^{ca}_{ik}$, $b^{nb'}_{ik}$=$-b^{ab}_{ik} - b^{bb}_{ik} - b^{cb}_{ik}$, $b^{nc'}_{ik}$=$-b^{ac}_{ik} - b^{bc}_{ik} - b^{cc}_{ik}$ and $b^{nn'}_{ik}$=$-b^{an}_{ik} - b^{bn}_{ik} - b^{cn}_{ik}$

$$\mathbf{G^*_{kk}} = \begin{bmatrix} g^{aa}_{kk} & g^{ab}_{kk} & g^{ac}_{kk} & g^{an}_{kk} \\ g^{ba}_{kk} & g^{bb}_{kk} & g^{bc}_{kk} & g^{bn}_{kk} \\ g^{ca}_{kk} & g^{cb}_{kk} & g^{cc}_{kk} & g^{cn}_{kk} \\ g^{na}_{kk} & g^{nb}_{kk} & g^{nc}_{kk} & g^{nn}_{kk} \\ g^{na'}_{kk} & g^{nb'}_{ik} & g^{nc'}_{kk} & g^{nn'}_{kk} - 1/r_k \end{bmatrix} \forall k \tag{12}$$

where $g^{na'}_{kk}$=$-g^{aa}_{kk} - g^{ba}_{kk} - g^{ca}_{kk}$, $g^{nb'}_{kk}$=$-g^{ab}_{kk} - g^{bb}_{kk} - g^{cb}_{kk}$, $g^{nc'}_{kk}$=$-g^{ac}_{kk} - g^{bc}_{kk} - g^{cc}_{kk}$ and $g^{nn'}_{kk}$=$-g^{an}_{kk} - g^{bn}_{kk} - g^{cn}_{kk}$. Notice that only one element of $\mathbf{G^*_{kk}}$ depends on the earthing resistance r_k. Matrices defined in equations 10-12 also depend on the elements of series and shunt 4-wire primitive admittances ($\widetilde{\mathbf{Y}}_{\mathbf{ik}}$=$\widetilde{\mathbf{G}}_{\mathbf{ik}}$+$\widetilde{\mathbf{B}}_{\mathbf{ik}}$i and $\widetilde{\mathbf{Y}}^{\mathbf{sh}}_{\mathbf{ik}}$=$\widetilde{\mathbf{B}}^{\mathbf{sh}}_{\mathbf{ik}}$i) constituting the fundamental blocks required to construct the Jacobian matrix of $\boldsymbol{h(x)}$, $\mathbf{H}$.

III. System State Estimation Formulation

The proposal is stated as a Weighted Least Squares (WLS) optimization problem as follows:

$$\min \quad [\widehat{\boldsymbol{z}} - \boldsymbol{h(x)}]^{\mathbf{T}} \cdot \mathbf{W} \cdot [\widehat{\boldsymbol{z}} - \boldsymbol{h(x)}] \tag{13}$$

where, $\boldsymbol{x}$ is a u-dimension vector of all system voltages and parameters to be estimated, hereafter called the *state of the system* vector. $\widehat{\boldsymbol{z}}$ is a m-dimension vector of field measurements. The hat symbol $\widehat{\cdot}$ denotes "measurement". $\boldsymbol{h(x)}$ is a m-dimension vector of the estimated values for each measurement in $\widehat{\boldsymbol{z}}$ according to the state of the system vector $\boldsymbol{x}$ and the 4-wire network model discussed in section II. $\mathbf{W}$ is a weight matrix whose diagonal is filled with the inverse squared variances of each voltage, current and resistance measuring device. The definition of technical characteristics and the minimum number of measuring devices to ensure observability is out of scope of the paper.

The state of the system vector $\boldsymbol{x}$ comprises 8 voltages per bus (corresponding to real and imaginary magnitudes for the three phases a, b, c and neutral n with respect to reference g at zero potential) and $n_b - 1$ earthing resistance parameters to be estimated (substation grounding mat resistance is excluded from the measurement vector). Thus, the total number of state variables is $u = 9n_b - 1$. The SSE problem is applied with the synchronized complex variables expressed in rectangular coordinates [1]. So, the state vector $\boldsymbol{x}$ is:

$$\boldsymbol{x} = [\boldsymbol{v^r}, \boldsymbol{v^i}, \boldsymbol{r}]^{\mathbf{T}} = [x_1, \ldots, x_u]^{\mathbf{T}} \tag{14}$$

where the system voltages $v^{q,r}_k = \Re[\overline{v}^q_k] \in \boldsymbol{v^r}$ and $v^{q,i}_k = \Im[\overline{v}^q_k] \in \boldsymbol{v^i}$ and $r_k \in \boldsymbol{r}$ is the $n_b - 1$-dimension vector.

The measurement vector $\widehat{\boldsymbol{z}}$ is decomposed in three parts: real and imaginary parts of PMU measured voltages and currents, and earthing resistance conventional or PMU measurements. Thus, the structure of $\widehat{\boldsymbol{z}}$ comprises the sets of all measurements phase to neutral voltages ($\widehat{\boldsymbol{v}}^{\boldsymbol{pn}}$), branch phase and neutral currents ($\widehat{\boldsymbol{f}}$), injected currents at all phases and neutrals ($\widehat{\boldsymbol{i}}$) and earthing resistance parameters ($\widehat{\boldsymbol{r}}$):

$$\widehat{\boldsymbol{z}} = [\widehat{\boldsymbol{v}}^{\boldsymbol{pn,r}}\widehat{\boldsymbol{v}}^{\boldsymbol{pn,i}}; \widehat{\boldsymbol{i}}^{\boldsymbol{r}}\widehat{\boldsymbol{i}}^{\boldsymbol{i}}; \widehat{\boldsymbol{f}}^{\boldsymbol{r}}\widehat{\boldsymbol{f}}^{\boldsymbol{i}}; \widehat{\boldsymbol{r}}]^{\mathbf{T}} = [z_1, \ldots, z_m]^{\mathbf{T}} \tag{15}$$

A maximum of 23 measurements per bus k could be considered, distributed in the following manner:

Three (3) real voltages: $\widehat{v}^{pn,r}_k$=$\widehat{v}^{p,r}_k - \widehat{v}^{n,r}_k$ for p=a, b, c.
Three (3) imaginary voltages: $\widehat{v}^{pn,i}_k$=$\widehat{v}^{p,i}_k - \widehat{v}^{n,i}_k$ for p=a, b, c.
Four (4) real branch currents: $\widehat{f}^{q,r}_k$ for q=a, b, c, n.
Four (4) imaginary branch currents: $\widehat{f}^{q,i}_{ik}$ for q=a, b, c, n.
Four (4) real injected currents: $\widehat{i}^{q,r}_{ik}$ for q=a, b, c, n.
Four (4) imaginary injected currents: $\widehat{i}^{q,i}_k$ for q=a, b, c, n.
One (1) earthing resistance: $\widehat{r}_k$.

The optimization problem should be stated in such a way that the number of measurements m has to be greater than the number of state variables u. Under a highly monitored scheme as stated above, the total of available measurements (m=$23n_b - 1$ and m=$15n_b - 1$ if branch currents are omitted) is sensibly higher than the number of state variables (u=$9n_b - 1$) guarantying a high degree of observability. In this case,

	∂v_1^r	∂v_i^r	∂v_k^r	$\partial v_{n_b}^r$	∂v_1^i	∂v_i^i	∂v_k^i	$\partial v_{n_b}^i$	∂r_1	∂r_i	∂r_k	∂r_{n_b}
$\partial v_1^{pn,r}$	$\mathbf{A}$	$\mathbf{O}$	$\mathbf{O}$	$\mathbf{O}$	$\mathbf{O}$	$\mathbf{O}$	$\mathbf{O}$	$\mathbf{O}$	$\boldsymbol{o}$	$\boldsymbol{o}$	$\boldsymbol{o}$	$\boldsymbol{o}$
$\partial v_i^{pn,r}$	$\mathbf{O}$	$\mathbf{A}$	$\mathbf{O}$	$\mathbf{O}$	$\mathbf{O}$	$\mathbf{O}$	$\mathbf{O}$	$\mathbf{O}$	$\boldsymbol{o}$	$\boldsymbol{o}$	$\boldsymbol{o}$	$\boldsymbol{o}$
$\partial v_k^{pn,r}$	$\mathbf{O}$	$\mathbf{O}$	$\mathbf{A}$	$\mathbf{O}$	$\mathbf{O}$	$\mathbf{O}$	$\mathbf{O}$	$\mathbf{O}$	$\boldsymbol{o}$	$\boldsymbol{o}$	$\boldsymbol{o}$	$\boldsymbol{o}$
$\partial v_{n_b}^{pn,r}$	$\mathbf{O}$	$\mathbf{O}$	$\mathbf{O}$	$\mathbf{A}$	$\mathbf{O}$	$\mathbf{O}$	$\mathbf{O}$	$\mathbf{O}$	$\boldsymbol{o}$	$\boldsymbol{o}$	$\boldsymbol{o}$	$\boldsymbol{o}$
$\partial v_1^{pn,i}$	$\mathbf{O}$	$\mathbf{O}$	$\mathbf{O}$	$\mathbf{O}$	$\mathbf{A}$	$\mathbf{O}$	$\mathbf{O}$	$\mathbf{O}$	$\boldsymbol{o}$	$\boldsymbol{o}$	$\boldsymbol{o}$	$\boldsymbol{o}$
$\partial v_i^{pn,i}$	$\mathbf{O}$	$\mathbf{O}$	$\mathbf{O}$	$\mathbf{O}$	$\mathbf{O}$	$\mathbf{A}$	$\mathbf{O}$	$\mathbf{O}$	$\boldsymbol{o}$	$\boldsymbol{o}$	$\boldsymbol{o}$	$\boldsymbol{o}$
$\partial v_k^{pn,i}$	$\mathbf{O}$	$\mathbf{O}$	$\mathbf{O}$	$\mathbf{O}$	$\mathbf{O}$	$\mathbf{O}$	$\mathbf{A}$	$\mathbf{O}$	$\boldsymbol{o}$	$\boldsymbol{o}$	$\boldsymbol{o}$	$\boldsymbol{o}$
$\partial v_{n_b}^{pn,i}$	$\mathbf{O}$	$\mathbf{O}$	$\mathbf{O}$	$\mathbf{O}$	$\mathbf{O}$	$\mathbf{O}$	$\mathbf{O}$	$\mathbf{A}$	$\boldsymbol{o}$	$\boldsymbol{o}$	$\boldsymbol{o}$	$\boldsymbol{o}$
∂f_{ik}^r	$\mathbf{O}$	$\widetilde{\mathbf{G}}_{\mathbf{ik}}^*$	$\widetilde{\mathbf{G}}_{\mathbf{ik}}^*$	$\mathbf{O}$	$\mathbf{O}$	$-\widetilde{\mathbf{B}}_{\mathbf{ik}}^*$	$-\widetilde{\mathbf{B}}_{\mathbf{ik}}^*$	$\mathbf{O}$	$\boldsymbol{o}$	$\boldsymbol{o}$	$\boldsymbol{o}$	$\boldsymbol{o}$
∂f_{ki}^r	$\mathbf{O}$	$-\widetilde{\mathbf{G}}_{\mathbf{ki}}^*$	$-\widetilde{\mathbf{G}}_{\mathbf{ki}}^*$	$\mathbf{O}$	$\mathbf{O}$	$\widetilde{\mathbf{B}}_{\mathbf{ki}}^*$	$\widetilde{\mathbf{B}}_{\mathbf{ki}}^*$	$\mathbf{O}$	$\boldsymbol{o}$	$\boldsymbol{o}$	$\boldsymbol{o}$	$\boldsymbol{o}$
∂f_{1k}^r	$\mathbf{O}$	$-\widetilde{\mathbf{G}}_{\mathbf{ik}}^*$	$-\widetilde{\mathbf{G}}_{\mathbf{ik}}^*$	$\mathbf{O}$	$\mathbf{O}$	$\widetilde{\mathbf{B}}_{\mathbf{ik}}^*$	$\widetilde{\mathbf{B}}_{\mathbf{ik}}^*$	$\mathbf{O}$	$\boldsymbol{o}$	$\boldsymbol{o}$	$\boldsymbol{o}$	$\boldsymbol{o}$
∂f_{k1}^r	$\mathbf{O}$	$\widetilde{\mathbf{G}}_{\mathbf{ki}}^*$	$\widetilde{\mathbf{G}}_{\mathbf{ki}}^*$	$\mathbf{O}$	$\mathbf{O}$	$-\widetilde{\mathbf{B}}_{\mathbf{ki}}^*$	$-\widetilde{\mathbf{B}}_{\mathbf{ki}}^*$	$\mathbf{O}$	$\boldsymbol{o}$	$\boldsymbol{o}$	$\boldsymbol{o}$	$\boldsymbol{o}$
∂i_1^r	$\mathbf{G}_{\mathbf{11}}^*$	$\mathbf{G}_{\mathbf{1i}}^*$	$\mathbf{G}_{\mathbf{1k}}^*$	$\mathbf{G}_{\mathbf{1n}}^*$	$-\mathbf{B}_{\mathbf{11}}^*$	$-\mathbf{B}_{\mathbf{1i}}^*$	$-\mathbf{B}_{\mathbf{1k}}^*$	$-\mathbf{B}_{\mathbf{1n}}^*$	$\boldsymbol{d_1}$	$\boldsymbol{o}$	$\boldsymbol{o}$	$\boldsymbol{o}$
∂i_i^r	$\mathbf{G}_{\mathbf{i1}}^*$	$\mathbf{G}_{\mathbf{ii}}^*$	$\mathbf{G}_{\mathbf{ik}}^*$	$\mathbf{G}_{\mathbf{in}}^*$	$-\mathbf{B}_{\mathbf{i1}}^*$	$-\mathbf{B}_{\mathbf{ii}}^*$	$-\mathbf{B}_{\mathbf{ik}}^*$	$-\mathbf{B}_{\mathbf{in}}^*$	$\boldsymbol{o}$	$\boldsymbol{d_i}$	$\boldsymbol{o}$	$\boldsymbol{o}$
∂i_k^r	$\mathbf{G}_{\mathbf{k1}}^*$	$\mathbf{G}_{\mathbf{ki}}^*$	$\mathbf{G}_{\mathbf{kk}}^*$	$\mathbf{G}_{\mathbf{kn}}^*$	$-\mathbf{B}_{\mathbf{k1}}^*$	$-\mathbf{B}_{\mathbf{ki}}^*$	$-\mathbf{B}_{\mathbf{kk}}^*$	$-\mathbf{B}_{\mathbf{kn}}^*$	$\boldsymbol{o}$	$\boldsymbol{o}$	$\boldsymbol{d_k}$	$\boldsymbol{o}$
$\partial i_{n_b}^r$	$\mathbf{G}_{\mathbf{n1}}^*$	$\mathbf{G}_{\mathbf{ni}}^*$	$\mathbf{G}_{\mathbf{nk}}^*$	$\mathbf{G}_{\mathbf{nn}}^*$	$-\mathbf{B}_{\mathbf{n1}}^*$	$-\mathbf{B}_{\mathbf{ni}}^*$	$-\mathbf{B}_{\mathbf{nk}}^*$	$-\mathbf{B}_{\mathbf{nn}}^*$	$\boldsymbol{o}$	$\boldsymbol{o}$	$\boldsymbol{o}$	$\boldsymbol{d_n}$
∂i_1^i	$\mathbf{B}_{\mathbf{11}}^*$	$\mathbf{B}_{\mathbf{1i}}^*$	$\mathbf{B}_{\mathbf{1k}}^*$	$\mathbf{B}_{\mathbf{1n}}^*$	$\mathbf{G}_{\mathbf{11}}^*$	$\mathbf{G}_{\mathbf{1i}}^*$	$\mathbf{G}_{\mathbf{1k}}^*$	$\mathbf{G}_{\mathbf{1n}}^*$	$\boldsymbol{e_1}$	$\boldsymbol{o}$	$\boldsymbol{o}$	$\boldsymbol{o}$
∂i_i^i	$\mathbf{B}_{\mathbf{i1}}^*$	$\mathbf{B}_{\mathbf{ii}}^*$	$\mathbf{B}_{\mathbf{ik}}^*$	$\mathbf{B}_{\mathbf{in}}^*$	$\mathbf{G}_{\mathbf{i1}}^*$	$\mathbf{G}_{\mathbf{ii}}^*$	$\mathbf{G}_{\mathbf{ik}}^*$	$\mathbf{G}_{\mathbf{in}}^*$	$\boldsymbol{o}$	$\boldsymbol{e_i}$	$\boldsymbol{o}$	$\boldsymbol{o}$
∂i_k^i	$\mathbf{B}_{\mathbf{k1}}^*$	$\mathbf{B}_{\mathbf{ki}}^*$	$\mathbf{B}_{\mathbf{kk}}^*$	$\mathbf{B}_{\mathbf{kn}}^*$	$\mathbf{G}_{\mathbf{k1}}^*$	$\mathbf{G}_{\mathbf{ki}}^*$	$\mathbf{G}_{\mathbf{kk}}^*$	$\mathbf{G}_{\mathbf{kn}}^*$	$\boldsymbol{o}$	$\boldsymbol{o}$	$\boldsymbol{e_k}$	$\boldsymbol{o}$
$\partial i_{n_b}^i$	$\mathbf{B}_{\mathbf{n1}}^*$	$\mathbf{B}_{\mathbf{ni}}^*$	$\mathbf{B}_{\mathbf{nk}}^*$	$\mathbf{B}_{\mathbf{nn}}^*$	$\mathbf{G}_{\mathbf{n1}}^*$	$\mathbf{G}_{\mathbf{ni}}^*$	$\mathbf{G}_{\mathbf{nk}}^*$	$\mathbf{G}_{\mathbf{nn}}^*$	$\boldsymbol{o}$	$\boldsymbol{o}$	$\boldsymbol{o}$	$\boldsymbol{d_n}$
∂r_1	$\boldsymbol{o}^{\mathbf{T}}$	$\boldsymbol{o}^{\mathbf{T}}$	$\boldsymbol{o}^{\mathbf{T}}$	$\boldsymbol{o}^{\mathbf{T}}$	$\boldsymbol{o}^{\mathbf{T}}$	$\boldsymbol{o}^{\mathbf{T}}$	$\boldsymbol{o}^{\mathbf{T}}$	$\boldsymbol{o}^{\mathbf{T}}$	1	0	0	0
∂r_i	$\boldsymbol{o}^{\mathbf{T}}$	$\boldsymbol{o}^{\mathbf{T}}$	$\boldsymbol{o}^{\mathbf{T}}$	$\boldsymbol{o}^{\mathbf{T}}$	$\boldsymbol{o}^{\mathbf{T}}$	$\boldsymbol{o}^{\mathbf{T}}$	$\boldsymbol{o}^{\mathbf{T}}$	$\boldsymbol{o}^{\mathbf{T}}$	0	1	0	0
∂r_k	$\boldsymbol{o}^{\mathbf{T}}$	$\boldsymbol{o}^{\mathbf{T}}$	$\boldsymbol{o}^{\mathbf{T}}$	$\boldsymbol{o}^{\mathbf{T}}$	$\boldsymbol{o}^{\mathbf{T}}$	$\boldsymbol{o}^{\mathbf{T}}$	$\boldsymbol{o}^{\mathbf{T}}$	$\boldsymbol{o}^{\mathbf{T}}$	0	0	1	0
∂r_{n_b}	$\boldsymbol{o}^{\mathbf{T}}$	$\boldsymbol{o}^{\mathbf{T}}$	$\boldsymbol{o}^{\mathbf{T}}$	$\boldsymbol{o}^{\mathbf{T}}$	$\boldsymbol{o}^{\mathbf{T}}$	$\boldsymbol{o}^{\mathbf{T}}$	$\boldsymbol{o}^{\mathbf{T}}$	$\boldsymbol{o}^{\mathbf{T}}$	0	0	0	1

Fig. 2. The structure of the Jacobian matrix: $\mathbf{H}$

the number of degrees of freedom grows with the number of monitored buses: d_f=$14n_b - 1$.

The measurement vector $\mathbf{h}(\mathbf{x})$ is defined as follows. For each measurement contained in $\widehat{z}_j \in \widehat{\boldsymbol{z}}$, $j = 1, \ldots, m$ there is a calculated value $h_j(\boldsymbol{x}) \in \boldsymbol{h}(\boldsymbol{x})$. The vector of calculated entries $\boldsymbol{h}(\boldsymbol{x})$ has the same structure of $\widehat{\boldsymbol{z}}$, that is:

$$\boldsymbol{h}(\boldsymbol{x}) = [\boldsymbol{v}^{\boldsymbol{pn,r}}\boldsymbol{v}^{\boldsymbol{pn,i}}; \boldsymbol{i}^{\boldsymbol{r}}\boldsymbol{i}^{\boldsymbol{i}}, \boldsymbol{f}^{\boldsymbol{r}}\boldsymbol{f}^{\boldsymbol{i}}; \boldsymbol{r}]^{\mathbf{T}} = [h_1, \ldots, h_m]^{\mathbf{T}} \quad (16)$$

Regarding neutral currents, measurements should be compared with two complex equations (4,5 and 7) simultaneously.

Terms $\boldsymbol{v}_{\boldsymbol{k}}^{\boldsymbol{pn,r}} \in \boldsymbol{v}^{\boldsymbol{pn,r}}$ and $\boldsymbol{v}_{\boldsymbol{k}}^{\boldsymbol{pn,i}} \in \boldsymbol{v}^{\boldsymbol{pn,i}}$ of $\boldsymbol{h}(\boldsymbol{x})$ can be directly obtained from the state vector as follows:

$$\boldsymbol{v}_{\boldsymbol{k}}^{\boldsymbol{pn,r}} = \left[\ \mathbf{A}\ \right][\boldsymbol{v}_{\boldsymbol{k}}^{\boldsymbol{r}}]^{\mathbf{T}} \quad \boldsymbol{v}_{\boldsymbol{k}}^{\boldsymbol{pn,i}} = \left[\ \mathbf{A}\ \right][\boldsymbol{v}_{\boldsymbol{k}}^{\boldsymbol{i}}]^{\mathbf{T}} \quad (17)$$

where $\mathbf{A}$ = [1 0 0 -1; 0 1 0 -1; 0 0 1 -1]. Terms $\boldsymbol{i}^{\boldsymbol{r}}$ and $\boldsymbol{i}^{\boldsymbol{i}}$ of $\boldsymbol{h}(\boldsymbol{x})$ are determined using Eq. 7. Terms $\boldsymbol{f}^{\boldsymbol{r}}$ and $\boldsymbol{f}^{\boldsymbol{i}}$ of $\boldsymbol{h}(\boldsymbol{x})$ are calculated from primitive series matrices $\widetilde{\mathbf{G}}_{\mathbf{ik}}$, $\widetilde{\mathbf{B}}_{\mathbf{ik}}$. Term $\boldsymbol{r}$ of $\boldsymbol{h}(\boldsymbol{x})$ is directly taken from the state of the system vector $\boldsymbol{x}$.

The structure of the Jacobian matrix ($\mathbf{H}$) of $\boldsymbol{h}(\boldsymbol{x})$ is shown in Fig. 2. Null matrices and vectors are expressed as $\mathbf{O}$ =zeros(4,5) and $\boldsymbol{o}$ =zeros(1,3) or $\boldsymbol{o}$ =zeros (1,5), respectively. Primitive series conductance and susceptance matrices $\widetilde{\mathbf{G}}_{\mathbf{ik}}$, $\widetilde{\mathbf{B}}_{\mathbf{ik}}$. Modified system conductance and susceptance matrices $\mathbf{G}_{\mathbf{ik}}^*$, $\mathbf{G}_{\mathbf{kk}}^*$, $\mathbf{B}_{\mathbf{ik}}^*$, $\mathbf{B}_{\mathbf{kk}}^*$ are given by Eqs. 10-12

The Jacobian matrix of $\boldsymbol{h}(\boldsymbol{x})$ ($\mathbf{H}$) is almost constant. $\mathbf{G}_{\mathbf{kk}}^*$=$\frac{\partial i_k^{n,r}}{\partial v_k^{n,r}}$= $\frac{\partial i_k^{n,i}}{\partial v_k^{n,i}}$ depends on r_k^{-1}. Derivatives $\frac{\partial r_k^{n,r}}{\partial r_k}$= $\boldsymbol{d_k}$ =[0, 0, 0, 0,v_k^r/r_k^2]$^{\mathbf{T}}$ and $\frac{\partial i_k^{n,i}}{\partial r_k}$= $\boldsymbol{e_k}$ =[0, 0, 0, 0,v_k^i/r_k^2]$^{\mathbf{T}}$ that also depends on r_k^{-2}, v_k^r and v_k^i.

Once defined the structure of the measurement vector $\boldsymbol{h}(\boldsymbol{x})$ and its Jacobian matrix $\mathbf{H}$, the optimization problem can be iteratively solved using any factorization method.

$$\boldsymbol{x}^{\nu+1} = \boldsymbol{x}^{\nu} + [\mathbb{G}(\boldsymbol{x}^{\nu})]^{-1}\mathbf{H}(\mathbf{x}^{\nu})^{\mathbf{T}}\mathbf{W}[\boldsymbol{h}(\boldsymbol{x}^{\boldsymbol{\nu}}) - \widehat{\boldsymbol{z}}] \quad (18)$$

where ν is the iteration index. The gain matrix $\mathbb{G}(\boldsymbol{x}^{\boldsymbol{\nu}})$=$\mathbf{H}(\mathbf{x}^{\nu})^{\mathbf{T}}\mathbf{W}\mathbf{H}(\mathbf{x}^{\nu})$ should not be inverted. It must be factorized if the system is fully observable. Finding out the best factorization method is out of the scope of the paper and matter of future research. The algorithm to solve Eq. 18 was coded in Matlab interpreter using the Cholesky decomposition and forward-backward substitution method [14]. The algorithm has seven steps:

1.- Start, set the iteration index ν=0.

2.- Initialize the state vector x^{ν}, usually as a flat start.

3.- Calculate the gain matrix, $\mathbb{G}(\boldsymbol{x}^{\boldsymbol{\nu}})$.

4.- Calculate the right hand side of Eq. 18

5.- Decompose $\mathbb{G}(\boldsymbol{x}^{\boldsymbol{\nu}})$ and solve for $\Delta\boldsymbol{x}^{\nu}$

6.- Test for convergence, $\max|\Delta\boldsymbol{x}^{\nu}|$=$|\boldsymbol{x}^{\nu+1} - \boldsymbol{x}^{\nu}| \leq \epsilon$.

7.- If no convergence, then update $\boldsymbol{x}^{\nu+1}$=$\boldsymbol{x}^{\nu}$+$\Delta\boldsymbol{x}^{\nu}$, and go to 3. Else, stop.

IV. Test Cases

The proposed distribution system state estimation formulation was applied using the well-known Kersting's Neutral-to-Earth Voltage (NEV) test system [16] and the IEEE NEV test case [7]. The Kersting NEV system was tested under two scopes. Firstly by using the original system topology with only two monitored buses (n_b = 2). In this scope, results can be easily replicated by the interested reader. Under the second scope the original Kersting's system topology is modified in order to be solved under large-scale conditions for different optimization problem sizes. To do so, the topology of the test system was stratified in l layers in order to get $n_b = 2^l$ monitored buses maintaining the same network structure and loading conditions. We define layer as a set of buses linked to the source with the same number of intermediate nodes. The method was also tested under real-world conditions using the IEEE NEV test system. Results were compared with the solutions provided by [2] and by [13].

A. Simple one-layer 2-bus NEV test system

The original system presented in [16] consists of a radial 4-wire (three-phase with neutral) main feeder connected to a 12.47 kV (line-to-line) source with an unbalanced load of $\overline{S}_L^a$+$\overline{S}_L^b$+$\overline{S}_L^c$ = 8.95$\angle$24.4^o MVA located at the farthest node.

The original NEV system has n_t = 21 buses. One generation node, one load node and 19 interconnecting nodes. Thus, to apply the method we reduce the system to n_b = 2 monitored buses [28]. The total length of the line is d_{12} = 6000 feet (1.13 miles). Line-to neutral voltages and injected currents (phase and neutral) are measured at starting and ending buses. At the substation, line neutral is connected to the ground mat (r_1 = 0.5 ohms). This resistance is not measured. From bus 2 to bus 20, the neutrals are not connected to ground, since there are no loads connected to those buses. At the load bus, neutral is grounded through a 5 ohm resistance (r_2 = 5.0 ohms) suitable to be measured.

The total number of measurements and state variables are m = $15n_b - 1$ = 29 (12 voltages, 16 currents and one resistance) and u = $8n_b$+1 = 17 (16 voltages and one resistance).

The set of unbiased measurements $\boldsymbol{z_0}$ was taken from the OpenDSS power flow script included in the GitHub page of the paper. Elements of $\boldsymbol{z_0}$ were randomly altered in order to get the set of m inaccurate measurements $\widehat{\boldsymbol{z}}$ according to the following equation:

$$\widehat{z}_j = z_{0j}(1 + n_l\mu) \tag{19}$$

where z_{0j} is the j measurement with no noise

n_l is the noise level in percent (3%, 6%, 9% and 12%)

μ is a sample of a uniformly distributed random variable in the interval [-1,1].

Voltage meter accuracy is assumed to be 3% of a 10kV scale. Phase current meter accuracy is assumed to be 3% of a 400A scale. Neutral current meter accuracy is assumed to be 3% of a 100A scale. Resistance meter accuracy is assumed to be 10% of a 5 ohm scale.

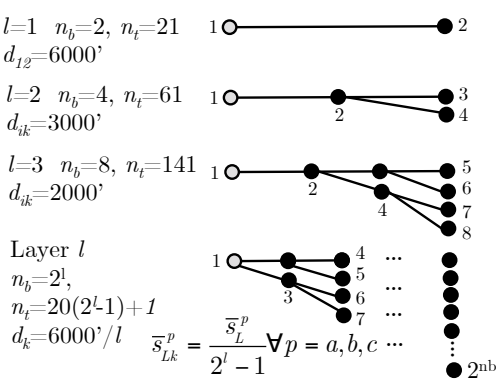

Fig. 3. Modified NEV test system

TABLE II
Structure of the Modified Kersting NEV test system

l	n_b	n_t	m	u	d_f
1	2	21	29	17	12
2	4	61	59	35	24
3	8	141	119	71	48
4	16	301	239	143	96
5	32	621	479	287	192
6	64	1261	959	575	
7	128	2541	1919	1151	758

B. Modified l-layer Kersting's NEV test system

The Kesting's NEV test system was extended from 2 to 128 monitored buses using a tree topology as shown in Fig. 3. The number of measured or monitored buses depends on the number of specified layers l, that is n_b=2^l. Total load (=8.95$\angle$24.4^o MVA) and main feeder length (6000') will remain unchanged at each layer. Line lengths and load magnitudes are resized according to the number of layers. Table II summarizes the structure of the modified NEV test system depending on the number of layers. For one layer (l=1), the system comprises u=17 state variables, m=29 measurements for n_t=21 buses where n_b=2 of them are monitored buses. Conversely, if l=7, the system comprises u=1151 state variables, m=1919 measurements for n_t=2541 buses where n_b=128 of them are monitored buses.

Notice that the test-system has high observability since the degrees of freedom (d_f) pass from 12 (layer 1) to 758 (layer 7). In this case all loads can be monitored. In real world, monitored buses are limited and a discussion about PMU location required. This aspect is not treated in this paper.

The set of biased measurements $\widehat{\boldsymbol{z}}$ is constructed from the set of unbiased measurements $\boldsymbol{z_0}$ randomly altered from a power flow solution using Eq. 19 for different noise levels n_l (3%, 6%, 9% and 12%). Unbiased system real power losses associated to power flow solutions at each layer l are also included in Table II.

The proposed SSE procedure is applied in all four feeders separately. Different type of measurements are considered: phase-to-neutral voltages, phase/neutral currents and pole earthing resistances. Each feeder has a different number of measurements, state variables and degrees of freedom accord-

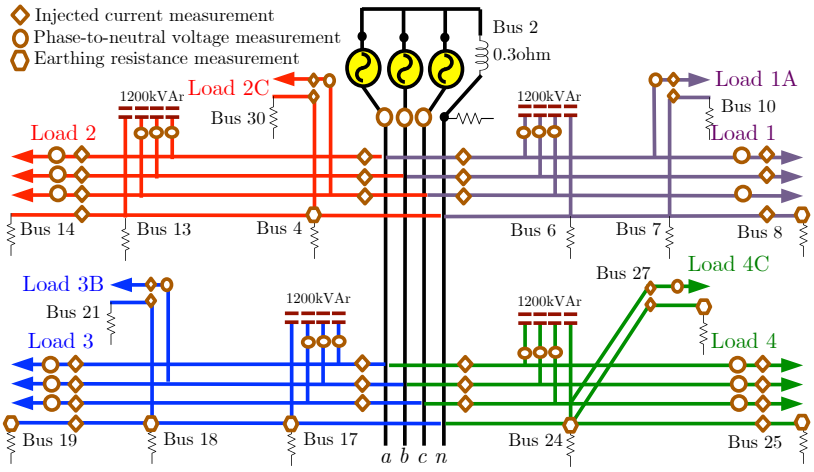

Fig. 4. IEEE NEV test system with PMU measurements [7].

TABLE III
IEEE NEV TEST CASE - FIELD PMU MEASUREMENTS

Feeder	Source bus						1-phase load				3-phase load								Capacitor				Splitting bus				SSE		
	Δv			i			Δv	i		R	Δv			i				R	Δv			R	Δv			R			
	an	bn	cn	a	b	c	an	a	n		an	bn	cn	a	b	c	n		an	bn	cn		an	bn	cn		m	u	df
1	2	2	2	2	2	2	2	2	2		2		2	2	2		2	1	2	2	2		2	2	2	1	44	32	10
2	2	2	2	2	2	2	2	2	2		2	2	2	2	2	2	2	1	2	2	2		2	2	2	1	46	32	14
3	2	2	2	2	2	2	2	2	2	1	2	2	2	2	2	2	2	1	2	2	2	1	2	2	2	1	48	32	16
4	2	2	2	2	2	2	2	2	2	1	2	2	2	2	2	2	2	1					2	2	2	1	41	27	14

ing to Table III.

C. The IEEE NEV test-system

The IEEE NEV test case is a 4-wire distribution system whose structure and topology details are found in [7]. The original IEEE NEV system is reduced from 80 to 16 buses (buses with zero power injections were eliminated). The multiphase line diagram of the reduced test case is shown in Fig 4. The pole earthing resistances at three-phase nodes 8, 14, 19 and 25 are 25, 15, 10 and 10 ohms, respectively. The ground resistances at single-phase nodes 10, 30, 21 and 27 are 25, 10, 50 and 50 ohms, respectively. The low voltage side of load transformers is not of interest in the test case.

Feeder 1 has 42 PMU measurements: 24 phase-neutral voltages (12 real and 12 imaginary voltages), 16 phase/neutral currents (8 real and 8 imaginary voltages) and 2 earthing resistances). In this case, phase-neutral voltage at bus 8, phase b, injected current at bus 8, phase c and earthing resistances at buses 6 and 10 are not measured variables. The state vector has 32 elements (14 real and 14 imaginary voltages and 4 resistances). Thus, the SSE problem comprises 10 degrees of freedom. The second, third and fourth feeders have 46, 48 and 41 PMU measurements, respectively.

The accuracy of the voltage meters is assumed to be σ=3% of a 10kV scale. Phase current meters accuracy is assumed to be σ=3% of a 400A scale. Neutral current meter accuracy is assumed to be σ=3% of a 100A scale. Resistance meter accuracy is assumed to be σ=9% of a 5 ohm scale. We used the solution for each feeder provided in [7] as base case tp get inaccurate measurements according to Eq. 19 with a noise level of n_l=5 %. Reduced admittance matrices $\mathbf{Y}$ and $\mathbf{Y_{BUS}}$ for each feeder were acquired from the OpenDSS solver.

V. RESULTS

In this section, the results of the application of the proposed SSE formulation over a number of test cases defined above are presented. In all cases, the convergence threshold is set as $\epsilon = 10^{-4}$.

A. Simple one-layer (2-bus) Kersting's NEV system

In this case, l is set equal to 1 layer and n_b = 2. A total of m = 29 measurements and u = 17 state variables are identified. We can recognize that $m > u$ with 12 degrees of freedom. The objective is to minimize the overall weighted squared error:

$$\min \quad \sum_{j=1}^{m=29} \frac{1}{\sigma_j^2}[\widehat{z}_j - h_j(\boldsymbol{x})]^2$$

The unbiased PMU measurement vector $\boldsymbol{z_0}$ is listed in the third column of Table IV. These values were taken from a power flow solution. The biased measurement vector $\widehat{\boldsymbol{z}}$ is listed in the fourth column of Table IV. These values were randomly obtained from Eq. 19 with a noise level of n_l = 3 %.

The results of the SSE are presented in Table IV (fifth column) where calculated measurements $\boldsymbol{h(x)}$ are given by $\boldsymbol{h(x)}$=$[\boldsymbol{v^{pn,r}v^{pn,i}}; \boldsymbol{i^r i^i}, \boldsymbol{r}]^{\mathbf{T}}$=$[h_1, h_2, ..., h_{29}]^{\mathbf{T}}$. According to Eq. 17 the first twelve rows (h_1-h_{12}) of $\boldsymbol{h(x)}$ are:

	∂v_1^r	∂v_2^r	∂v_1^i	∂v_2^i	∂r_2
$\partial v_1^{pn,r}$	$\mathbf{A}$	$\mathbf{O}$	$\mathbf{O}$	$\mathbf{O}$	$\boldsymbol{o}$
$\partial v_2^{pn,r}$	$\mathbf{O}$	$\mathbf{A}$	$\mathbf{O}$	$\mathbf{O}$	$\boldsymbol{o}$
$\partial v_1^{pn,i}$	$\mathbf{O}$	$\mathbf{O}$	$\mathbf{A}$	$\mathbf{O}$	$\boldsymbol{o}$
$\partial v_2^{pn,i}$	$\mathbf{O}$	$\mathbf{O}$	$\mathbf{O}$	$\mathbf{A}$	$\boldsymbol{o}$
∂i_1^r	$\mathbf{G_{11}^*}$	$\mathbf{G_{12}^*}$	$-\mathbf{B_{11}^*}$	$-\mathbf{B_{12}^*}$	$\boldsymbol{o}$
∂i_2^r	$\mathbf{G_{21}^*}$	$\mathbf{G_{12}^*}$	$-\mathbf{B_{21}^*}$	$-\mathbf{B_{22}^*}$	$\boldsymbol{d_2}$
∂i_1^i	$\mathbf{B_{11}^*}$	$\mathbf{B_{12}^*}$	$\mathbf{G_{11}^*}$	$\mathbf{G_{12}^*}$	$\boldsymbol{o}$
∂i_2^i	$\mathbf{B_{21}^*}$	$\mathbf{B_{22}^*}$	$\mathbf{G_{i2}^*}$	$\mathbf{G_{22}^*}$	$\boldsymbol{e_2}$
∂r_2	$\boldsymbol{o}^{\mathbf{T}}$	$\boldsymbol{o}^{\mathbf{T}}$	$\boldsymbol{o}^{\mathbf{T}}$	$\boldsymbol{o}^{\mathbf{T}}$	1

Fig. 5. 2-bus NEV system - Jacobian matrix ($\mathbf{H}$) structure

$$\begin{bmatrix} h_1 \\ h_2 \\ \vdots \\ h_{12} \end{bmatrix} = \begin{bmatrix} \boldsymbol{v_1^{pn,r}} & \mathbf{A} \\ \boldsymbol{v_1^{pn,i}} & \mathbf{A} \\ \boldsymbol{v_2^{pn,r}} & \mathbf{A} \\ \boldsymbol{v_2^{pn,i}} & \mathbf{A} \end{bmatrix} \tag{20}$$

Rows h_{13}-h_{28} are obtained according to Eq. 7:

$$\begin{bmatrix} h_{13} \\ h_{14} \\ \vdots \\ h_{28} \end{bmatrix} = \begin{bmatrix} \boldsymbol{i_1^r} \\ \boldsymbol{i_2^r} \\ \boldsymbol{i_1^i} \\ \boldsymbol{i_2^i} \end{bmatrix} = \begin{bmatrix} \mathbf{G_{11}^*} & \mathbf{G_{12}^*} & -\mathbf{B_{11}^*} & -\mathbf{B_{12}^*} \\ \mathbf{G_{21}^*} & \mathbf{G_{22}^*} & -\mathbf{B_{21}^*} & -\mathbf{B_{22}^*} \\ \mathbf{B_{11}^*} & \mathbf{B_{12}^*} & \mathbf{G_{11}^*} & \mathbf{G_{12}^*} \\ \mathbf{B_{21}^*} & \mathbf{B_{22}^*} & \mathbf{G_{21}^*} & \mathbf{G_{22}^*} \end{bmatrix} \begin{bmatrix} \boldsymbol{v_1^r} \\ \boldsymbol{v_2^r} \\ \boldsymbol{v_1^i} \\ \boldsymbol{v_2^i} \end{bmatrix}$$

where $\mathbf{G_{22}^*}$ is determined according to Eq. 12). Note that all equations of $\boldsymbol{h(x)}$ have constant parameters excepting rows h_{20} and h_{28} on which element (4,4) of $\mathbf{G_{22}^*}$(Eq. 12) depends on r_2 value at each iteration. The last row solution ($h_{29} = r_2$) is directly taken from the seventeenth element of the state vector $x_{17} \in \boldsymbol{x}$. Measured real and imaginary parts of the neutral currents should be compared with two complex equations given by 4,5 and 7 representing the calculated neutral currents. Thus, four rows (16b, 20b, 24b and 28b) must be added.

The weightings $W_j = \sigma_j^{-2}$ are included in Table IV (sixth column) according to the standard deviations of the measurement devices previously defined in Section IV. The structure of the state vector is given by $\boldsymbol{x}$=$[\boldsymbol{v^r}, \boldsymbol{v^i}, \boldsymbol{r}]^{\mathbf{T}} = [x_1, x_2, ..., x_{17}]^{\mathbf{T}}$, where $\boldsymbol{v^r} = [v_1^{a,r}, v_1^{b,r}, v_1^{c,r}, v_1^{n,r}, \ v_2^{a,r}, v_2^{b,r}, v_2^{c,r}, v_2^{n,r}]^{\mathbf{T}}$, $\boldsymbol{v^i}$=$[v_1^{a,i}, v_1^{b,i}, v_1^{c,i}, v_1^{n,i}, \ v_2^{a,i}, v_2^{b,i}, v_2^{c,i}, v_2^{n,i}]^{\mathbf{T}}$ and $\boldsymbol{r} = [r_2]^{\mathbf{T}}$. The last column of Table IV corresponds to the residual of each measurement $\sigma_j^{-2}{\Delta z_j}^2$.

The structure of the Jacobian matrix ($\mathbf{H}$) of $\boldsymbol{h(x)}$ is depicted in Fig. 5. Size of $\mathbf{H}$ is 33x17. Only four elements of $\mathbf{H}$ (2.4 %) will change their value at each iteration: Element (4,4) of $\mathbf{G_{22}^*}$ (twice), the fourth element of $\boldsymbol{d_2}$=$[0,0,0,0,v_2^r/r_2^2]^{\mathbf{T}}$ and the fourth element of $\boldsymbol{e_2}$=$[0,0,0,0,v_2^i/r_2^2]^{\mathbf{T}}$.

Fig. 6 shows the state vector $\boldsymbol{x}$ obtained from Eq. 18. The results are expressed in polar coordinates in order to compare voltage and current angles with the PMU reference θ_0=0.

The results of the SSE are summarized as follows. Overall residual J is 2.62. Estimated earthing resistance is 4.949 ohms, (actually, the ground resistance is 5.0 ohms). Estimated neutral and residual current are around f_{12}^n = 147.1 A and f_{12}^g = 25.4 A (no noise neutral and residual currents are 145.35 A and 26.34 A). Neutral to earth voltage (NEV) at bus 2 is v_2^n = 134.4 V (no noise NEV is 131.7 V).

TABLE IV
2-BUS NEV SYSTEM - MEASUREMENT VECTOR RESULTS FOR n_l= 3 %

j	Variable	z_{0j}	$\widehat{z}_j$	h_j	$\sigma_j^{-2} \in \mathbf{W}$	$\sigma_j^{-2}{\Delta z_j}^2$
1	$v_1^{an,r}$,V	5088	5137	5197	11.1	0.0406
2	$v_1^{bn,r}$,V	1720	1716	1720	11.1	0.0001
3	$v_1^{cn,r}$,V	-6853	-6737	-6791	11.1	0.0315
4	$v_2^{an,r}$,V	4829	4995	4934	11.1	0.0406
5	$v_2^{bn,r}$,V	1243	1242	1239	11.1	0.0001
6	$v_2^{cn,r}$,V	-6737	-6729	-6676	11.1	0.0315
7	$v_1^{an,i}$,V	4950	5000	5037	11.1	0.0154
8	$v_1^{bn,i}$,V	-6884	-6690	-6885	11.1	0.4223
9	$v_1^{cn,i}$,V	1907	1864	1859	11.1	0.0003
10	$v_2^{an,i}$,V	4556	4680	4643	11.1	0.0154
11	$v_2^{bn,i}$,V	-6717	-6909	-6714	11.1	0.4223
12	$v_2^{cn,i}$,V	1986	1930	1935	11.1	0.0003
13	$i_1^{a,r}$,A	431	431	432	6944.4	0.0131
14	$i_1^{b,r}$,A	-69	-70	-72	6944.4	0.0350
15	$i_1^{c,r}$,A	-237	-234	-235	6944.4	0.0076
16a	$i_1^{n,r}$,A	-99	-101	-101	1.11E+05	0.0005
16b	$i_1^{n,r}$,A	-99	-101	-100	1.11E+05	0.1160
17	$i_2^{a,r}$,A	-431	-439	-432	6944.4	0.3302
18	$i_2^{b,r}$,A	69	69	72	6944.4	0.0714
19	$i_2^{c,r}$,A	237	230	235	6944.4	0.1389
20a	$i_2^{n,r}$,A	99	98	98	1.11E+05	0.0000
20b	$i_2^{n,r}$,A	99	98	100	1.11E+05	0.3100
21	$i_1^{a,i}$,A	136	139	136	6944.4	0.0728
22	$i_1^{b,i}$,A	-507	-513	-512	6944.4	0.0099
23	$i_1^{c,i}$,A	265	263	268	6944.4	0.1235
24a	$i_1^{n,i}$,A	107	108	107	1.11E+05	0.0025
24b	$i_1^{n,i}$,A	107	108	108	1.11E+05	0.0534
25	$i_2^{a,i}$,A	-136	-134	-136	6944.4	0.0322
26	$i_2^{b,i}$,A	507	510	512	6944.4	0.0314
27	$i_2^{c,i}$,A	-265	-273	-268	6944.4	0.2013
28a	$i_2^{n,i}$,A	-107	-109	-109	1.11E+05	0.0000
28b	$i_2^{n,i}$,A	-107	-109	-108	1.11E+05	0.0545
29	r_2,Ω	5.00	4.95	4.95	4.9	0.0000
					$J(\boldsymbol{x})$=	2.6275

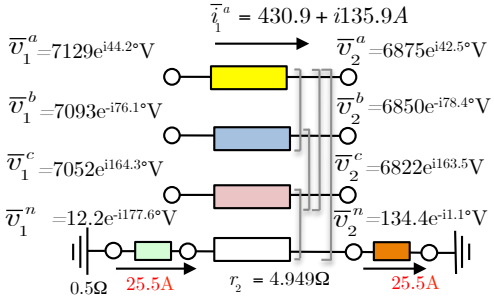

Fig. 6. 2-bus NEV system - State of the system for n_l= 3 %

Validation of the results: The results obtained using the normal-equation formulation were validated with the results of applying a general purpose optimization procedure. Results coincide. The main difference observed lies in the convergence time. The normal equation solution requires about 2.12 ms to converge while the Matlab's *fmincon* needs almost 112 ms to converge. Solutions from an Excel worksheet were also included in the GitHub page.

Bad data detection: The results of the state estimator provide valuable information to detect measurement errors,

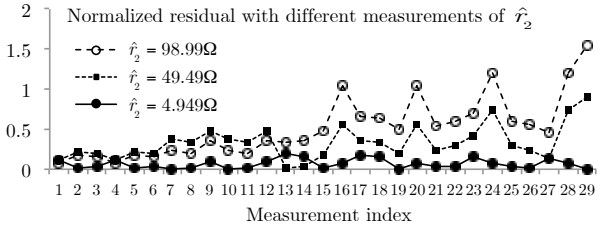

Fig. 7. 2-bus NEV system - Normalized residuals with different $\hat{r}_2$

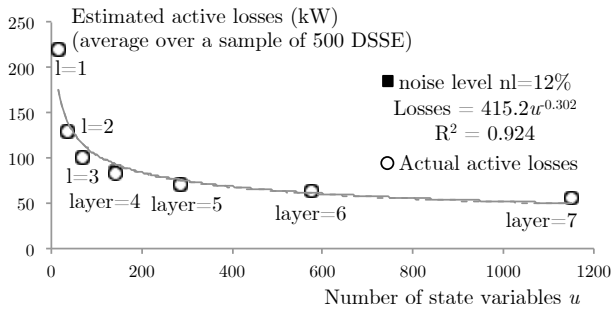

Fig. 8. Large-scale - Losses from 17 (layer 1) to 1151 (layer 7) state variables

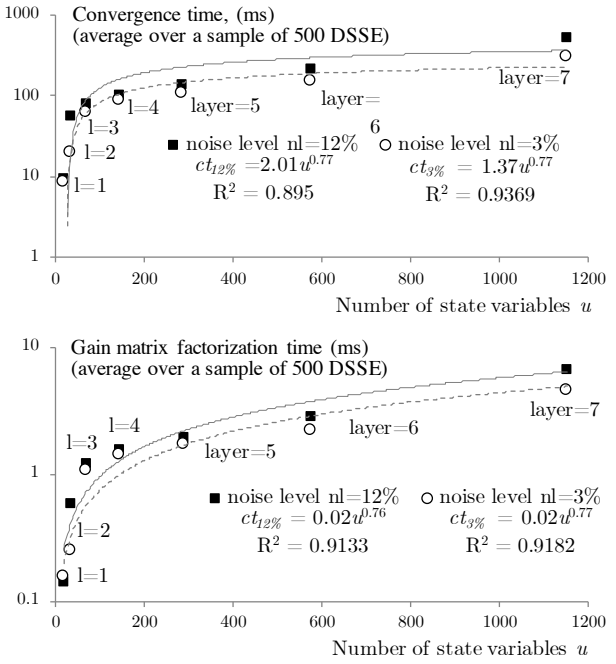

Fig. 9. Large-scale - CPU times from 17 (l=1) to 1151 (l=7) state variables

identify and eliminate them if possible. The chi-square test aims to find the confidence level of the dataset through the p-value (pV) of the weighted squared residual $J(\boldsymbol{x})$. No suspicious data is found if pV is closer to 100 %. In this case, for a noise level of n_l = 3 %, a residual $J(\boldsymbol{x})$ = 2.62 and df=$m - u$ = 12 degrees of freedom, the p-value is $pV_{12,2.62} = \int_{2.62}^{\infty} \chi^2_{12}(a)da$ = 99.77 %. Therefore, we observe no suspicious data for n_l = 3 %.

Bad data identification: We use normalized residuals [14] for bad data detection and identification. A bad measurement value is intentionally introduced in the dataset to test the identification method. Figure 7 shows normalized residuals when the resistance measurement is intentionally altered. Resulting residuals are clearly sensible to errors at voltages inaccuracies.

Comparison study with a PMU linear model: The proposal was compared with a linear three-phase PMU-SSE whose formulation can be found in [2]. Real power losses are estimated in the test-case (Section IV) varying the earthing resistance from r_2=1 Ω to r_2=250 Ω. The resulting power losses for the 4-wire non-linear SSE ranged from 220 kW (1 Ω) to 240 kW (250 Ω). The linear SSE approach always yields losses by 192kW since this method does not include any representation for earthing resistances. This result demonstrates how inaccuracies in the ground loop parameters can affect the estimations. Observe in results that losses are 10 % higher than the linear ones when using a complete 4-wire model.

B. Large-scale application: l-layer Kersting's NEV system

The Kesting's NEV test system was extended from 2 (layer l = 1) to 128 (layer l = 7) monitored buses using the methodology described in section IV-B. Thus, the proposal will be evaluated considering gain matrix sizes from 289 (l = 1) to 1324801 (l = 7) elements and Jacobian matrix sizes from 493 (l = 1) to 2208769 (l = 7) elements. The optimization model was scripted and run under Matlab interpreter using an Apple MacBookPro Core-2 Duo 1.7GHz Intel-i7 with 16 MB RAM. The model was executed 500 times in order to get average estimated power losses, p-values and performance times for different errors: n_l = 0, 3, 6, 9, 12 % and layers: for l = 1,u = 17 to l = 7, u =1151. In all cases, the system is highly observable as discussed in section IV-B. The degrees of freedom vary from d_f = 12 (l = 1) to d_f = 768 (l = 7).

Figures 8 and 9 display technical and performance results, the power losses obtained and the computer processing times across large-scale specified sizes. For the sake of clarity only two simulations with measurement noise of n_l = 3 % and n_l = 12 % are depicted.

As a result of the tree topology of the test-case, losses are naturally decreasing with the number of layers. We observe that at layer 1 (n_b = 2, u = 17), estimated losses are 220.7 kW (n_l = 3 %) and 222.37 kW (n_l = 12 %) whereas the actual ones are 220.8 kW. The difference is small (0.009 %). Regarding layer 7 (n_b = 128, u = 1151), estimated losses are 55.45 kW (n_l = 3 %) and 55.63 kW (n_l= 12 %) whereas the actual losses are 55.35 kW. In this case, if a noise level of 12 % is introduced in the data set, the difference between estimated and actual losses is about 2.3 %. The last result seems to be reasonable. However, the results of bad-data detection tests displayed in Table V show p-values near to zero when the noise is high. Thus, bad data is suspected. The p-values included in Table V were determined for l = 1, 3, 5, 7 and n_l = 0, 3, 6, 9 and 12 %.

The algorithm shows a fast convergence. The results also indicate that the presence of inaccurate measurements tends to deteriorate the convergence rate. The overall average time to get convergence goes from 10.2 ms (layer 1, u = 17, n_l= 3 %) to 313.6 ms (layer 7, u = 1151, n_l = 12 %). Convergence

TABLE V
LARGE-SCALE - BAD-DATA DETECTION: PVALUE: $pV_{df,J(l,n_l)}$

Noise Level	l=1 $pV_{12,J}$	l=3 $pV_{48,J}$	l=5 $pV_{192,J}$	l=7 $pV_{768,J}$
0%	100.00 %	100.00 %	100.00 %	100.00
3%	99.18 %	100.00 %	100.00 %	100.00
6%	50.15 %	99.99 %	100.00 %	100.00
9%	8.68 %	83.56 %	98.84 %	100.00
12%	0.79 %	13.46 %	1.95 %	0.00

TABLE VI
IEEE NEV TEST CASE - STATE OF THE SYSTEM: EARTHING RESISTANCES AND SINGLE-PHASE VOLTAGES

var	NEV SSE	4-wire SSE [13]	Linear SSE [2]
		Feeder No. 4	
v_{27}^b	7700.06	7709.66	7682.87
v_{27}^n	45.54	29.10	-
θ_{27}^b	-124.50	-124.69	-124.28
θ_{27}^n	-126.40	-114.16	-
R_{24}	100.76	-	-
R_{25}	9.76	-	-
R_{27}	49.65	-	-

time functions are $ct_{3\%} = 2.01u^{0.76}$ and $ct_{12\%} = 1.37u^{0.77}$.

Focusing on the average time to solve the normal equation (Eq. 18), gain matrix factorization time goes from 0.19 ms (layer 1: u = 17, n_l = 3 %) to 6.6 ms (layer 7: u = 1151, n_l = 12 %). Convergence time functions for the gain matrix factorization are $ct_{3\%} = 0.020u^{0.76}$ and $ct_{12\%} = 0.029u^{0.77}$. We must refer that 6.6 ms to solve a system of 1151 state variables is competitive on account of the use of an interpreter processor as Matlab.

The results discussed above illustrate the applicability of this proposal in the real world. The interested reader can replicate the results of all power flows and the proposed state estimator by executing the Matlab and Octave scripts provided in https://github.com/pmdeoliveiradejesus/4wire-WLS-PMU-DSSE.

Finally, concerning the limitations of this proposal, the quality of the results, as in other applications, will depend on a credible network model. The convergence behavior of the SSE is strongly affected by topology errors. Therefore, preprocessing tasks, such as topology and phase identification, are necessary to ensure a credible admittance matrix. These preprocessing tasks were not included in this initial approach. In the real-world, the PMUs are located at a limited number of MV/LV transformer points, not enough to ensure observability. Future work should apply the proposed SSE for fault detection and localization considering also the aggregation smart meter measurements at LV loads in order to decrease as much as possible the number of PMUs.

C. The IEEE Neutral-Earth Voltage (NEV) test system

The proposed method was also applied in the IEEE Neutral-Earth Voltage (NEV) test system [7]. Results obtained were compared with solutions provided by two existing state estimation procedures: the three-phase linear SSE [2] and the 4-wire SSE method recently introduced by [13]. The procedures were applied with the same loading conditions but differences depending on each model features and limitations.

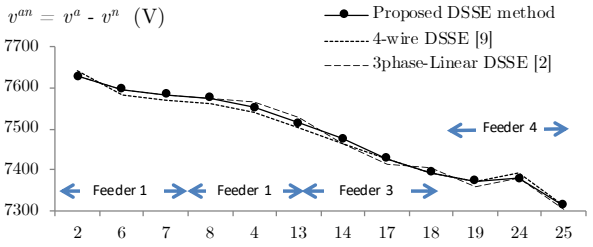

Fig. 10. IEEE NEV system - Phase a-Neutral voltage with and without the earthing resistance as state variable

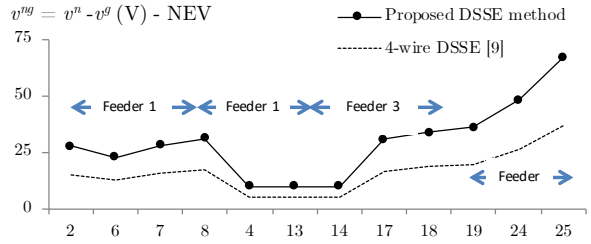

Fig. 11. IEEE NEV system - Neutral-Earth voltage with and without the earthing resistance as state variable

As a key contribution, the proposed SSE method incorporates earthing resistances as both state variables and field measurements. Random errors were introduced in measured earthing resistances considering a noise level of n_l=5 % (Eq. 19) with respect to the actual resistance values previously defined in section IV-C. The 4-wire SSE method [13] does not include earthing resistances as measurements or state variables in the problem formulation. Neutral conductor impedances and earthing resistances are regarded as fixed and known parameters whose value should be estimated offline. Therefore, as these resistances vary according to a number of external parameters (temperature, moisture, etc.), the ground loop parameters might be under or overestimated. When applying the 4-wire SSE method, we assume that earthing resistance magnitude is 50 % below than the actual resistances (with no noise) defined in section IV-C. Finally, the three-phase linear SSE method [2] does not include any ground loop representation working only with the 3x3 impedances matrices obtained from primitive impedance matrices via Kron's reduction.

Figures 10 and 11 show the resulting phase a to neutral voltage and neutral to earth voltage (NEV) estimation at main three-phase trunk of each feeder at buses 2, 6, 7, 8, 4, 13, 14, 17, 18, 19, 24, and 25. Estimations for phases b and c are not included due to space constraints. Resulting single-phase a to neutral voltages associated with laterals and estimated earthing resistances are listed in Table VI. Due to lack of space only results for feeder No. 4 are presented in this table.

We observe similar results when comparing the estimated steady-state magnitudes for the phase-to-neutral voltages in the three applied methods. However, significant differences are seen if we compare the resulting neutral to earth voltages between our proposal and the 4-wire SSE method [13]. We must point out that the three-phase linear SSE method cannot

estimate neutral to earth voltages [2].

As we modeled earthing resistances of the 4-wire DSEE method with an underestimation of 50 %, resulting NEVs are also clearly underestimated. In general, it is hard to find an appropriate value for the earthing resistances in the modeling stage of the SSE. This proposal overcomes the inaccuracy inherent in grounding parameters allowing us to evaluate how neutral voltage displacements and compare them with the system safety requirements such as [6].

VI. Conclusions

Existing System State Estimation (SSE) procedures have no observability of neutral-earth voltages associated to unbalanced distribution systems. In next generation distribution systems the use of PMU infrastructure to measure phase/neutral voltages, currents and earthing resistances, as well as appropriate multiphase multi-grounded network models, can provide high-speed visibility with an accurate and reliable model.

As a key contribution, this paper incorporates earthing resistances as both state variables and field measurements in the optimization problem. Operation and protection engineers will benefit of enhanced observability allowing to prevent equipment and personal losses due to temporary overvoltages under steady-state and fault conditions. The method was successfully tested under large-scale conditions.

The WLS method was used for didactic purposes. We encourage the use and further development of the methodology considering different SSE approaches.

References

[1] G. T. Heydt, "The next generation of power distribution systems," *IEEE Trans. on Smart Grid*, vol. 1 no. 3, pp. 225-235, 2010.

[2] M. Kezunovic, S. Meliopoulos, V. Venkatasubramanian, *Application of time-synchronized measurements in power system transmission networks*, Berlin, Springer, 2014.

[3] H. Mohsenian-Rad, et al, "Distribution synchrophasors," *IEEE Power Energy Mag.*, vol. 13, no. 3, pp. 26-34, 2018.

[4] R. Dugan and D. Montenegro, *The Open Distribution System Simulator (OpenDSS) - Reference Guide*, Electric Power Research Institute, 2019.

[5] P. M. De Oliveira-De Jesus, C. H. Antunes, "A detailed network model for distribution systems with high penetration of renewable generation sources," *Electric Power Systems Research*, vol. 161, pp. 152-166, 2018.

[6] "IEEE Guide for Safety in AC Substation Grounding," *in IEEE Std 80-2013*, pp.1-226, 2014

[7] R. Dugan, S. Carneiro, L. Ramos, D. Penido, "Neutral-to-Earth Voltage (NEV) Test Case," IEEE PES Test Feeders. Available at: https://site.ieee.org/pes-testfeeders/resources/

[8] Laepple, Klaus. "Method of measuring earth ground resistance of a pylon," U.S. Patent No. 9 239 352, Jan. 19, 2016.

[9] A. Phillips, *Future Inspection of Overhead Transmission Lines*, Electric Power Research Institute: Palo Alto, CA, USA, 2008.

[10] Y. Liu, L. Wu, J. Li, "D-PMU based applications for emerging active distribution systems A review," *Electric Power Systems Research*, vol. 179, p. 106063, 2020

[11] A. Primadianto and C. Lu, "A review on distribution system state estimation," *IEEE Trans. on Power Syst.*, vol. 32 no. 5, pp. 3875-3883, 2017.

[12] K. Dehghanpour, Z. Wang, J. Wang, Y. Yuan and F. Bu, "A Survey on State Estimation Techniques and Challenges in Smart Distribution Systems," *IEEE Trans. on Smart Grid*, vol. 10, no. 2, pp. 2312-2322, 2019.

[13] Y. Liu, J. Li, L. Wu, "State Estimation of Three-Phase Four-Conductor Distribution Systems with Real-Time Data from Selective Smart Meters," *IEEE Trans. on Power Syst.*, vol. 34, no. 4, pp. 2632-2843, 2019.

[14] A. Gomez-Exposito and A. Abur, *Power system state estimation: theory and implementation*, FL, USA: CRC press, 2004.

[15] W. Kersting, *Distribution system modeling and analysis*, FL, USA: CRC press, 2018

[16] W.H. Kersting, "A three-phase unbalanced line model with grounded neutrals through a resistance," *In Proc. IEEE PESGM'08*, p, 1-6, 2008

[17] S.T. Mak, "Smart meters serving as synchro-sensors for Smart Distribution Grid applications," *in Power and Energy Society General Meeting*, San Diego, CA., 2011, pp. 1-3

[18] D.A. Haughton and G.T. Heydt, "A Linear State Estimation Formulation for Smart Distribution Systems," *IEEE Trans. Power Syst.*, vol. 28, no. 2, pp. 1187-1195, 2013

[19] M. Pau, P. A. Pegoraro and S. Sulis. "Efficient branch-current-based distribution system state estimation including synchronized measurements," *IEEE Transactions on Instrumentation and Measurement* vol. 62 no. 9 pp. 2419-2429, 2013.

[20] X. Kong, Y. Chen, T. Xu, C. Wang, C. Yong, P. Li, L. Yu "A hybrid state estimator based on SCADA and PMU measurements for MV distribution system," *Applied Sciences*, vol. 8, no. 9, pp. 1527, 2018

[21] Y. Chen, X. Kong, C. Yong, X. Ma, and L. Yu, "Distributed State Estimation for Distribution Network with Phasor Measurement Units Information," *Energy Procedia*, vol. 158 pp. 4129-4134, 2019

[22] F. F. Wu and A. F. Neyer, Asynchronous distributed state estimation for power distribution systems, in *Proc. 10th PSCC*, pp. 439-446, 1990

[23] I. Roytelman and S. M. Shahidehpour, State estimation for electric power distribution systems in quasi real-time conditions, *IEEE Trans. Power Del.*, vol. 8, no. 4, pp. 2009-2015, 1993

[24] M. E. Baran and A. W. Kelley, "A branch current based state estimation method for distribution systems," *IEEE Trans. Power Syst.*, vol. 10, no. 1, pp. 483-491, 1995.

[25] C. N. Lu, J. H. Teng, and W. H. Liu, "Distribution system state estimation." *IEEE Trans. on Power Syst.* vol. 10, no. 1, pp. 229-240, 1995.

[26] J. Wu, Y He, and N Jenkins, "A robust state estimator for medium voltage distribution networks," *IEEE Trans. Power Syst.*, vol. 28, no. 2, pp. 1008- 1016, 2012.

[27] M. Gol and A. Abur, LAV based robust state estimation for systems measured by PMUs, *IEEE Trans. Smart Grid*, vol. 5, no. 4, pp. 1808 1814, 2014.

[28] P. M. De Oliveira-De Jesus and A. A. Rojas-Quintana, "Distribution system state estimation model using a reduced quasi-symmetric impedance matrix," *IEEE Trans. on Power Syst.*, vol. 30, no. 6, pp. 2856-2866, 2015.

[29] I. Dzafic, R. A. Jabr, I. Huseinagic, B. C. Pal, "Multi-phase state estimation featuring industrial-grade distribution network models," *IEEE Trans. Smart Grid*, vol. 8, no. 2, pp. 609618, 2017.

[30] Y. Zhang, J. Wang and Z. Li,, "Interval State Estimation with Uncertainty of Distributed Generation and Line Parameters in Unbalanced Distribution Systems," in *IEEE Trans. Power Syst.*

[31] B. R. Pokhrel, B. Bak-Jensen, and J. R. Pillai "Integrated Approach for Network Observability and State Estimation in Active Distribution Grid," *Energies* vol. 12, no. 12, pp. 2230, 2019.

[32] T. Chen, L. Sun, K. Ling, and W. K. Ho, , "Robust Power System State Estimation Using t-Distribution Noise Model," *in IEEE Syst. Journal*, vol. 14, no. 1 pp. 771-781, 2020

P. M. De Oliveira De Jesus (M'03, SM'14) received the M.Sc. and the Electrical Engineering (5 year course) degree in 2002 and 1.995 from Universidad Simón Bolívar (USB), Caracas, Venezuela, and Ph.D. (2008) degree from Oporto University, Portugal. Postdoctoral research at Coimbra University, Portugal in 2014-2015. Former head of the USB's Energy Institute. Associate professor 2007-2014. Full professor2014-2016. Currently he is visiting professor with the Department of Electrical Engineering, School of Engineering, Universidad de Los Andes, Colombia. His research interests include technical and economic issues of electric power and energy systems.

N.A. Rodriguez Received the electrical engineer degree from the Universidad de los Andes in 2019. His current research interest is focused in power system analysis and state estimation.

D. F. Celeita (SM'2019) received the degree in Electronic Engineering (2011) from Universidad Distrital Francisco Jos de Caldas, Bogot, Colombia and M.Sc. (2014) and Ph.D (2018) in Electrical Engineering from Universidad de los Andes, Bogota, Colombia. He worked as an automation engineer in low and medium voltage applications for a few years. He was a visiting researcher at Georgia Institute of Technology and he served as a postdoctoral researcher at CentraleSuplec with an industry partner in France. He is currently a Postdoctoral Research Associate at Universidad de los Andes. His research interest includes Protective - Relaying Control, Smart Grids, Advanced Distribution Automation, Fault Location, and Real-Time Simulation.

G.A. Ramos (M'04 - SM'13) received the degree in Electrical Engineering (1997) from Universidad Nacional, Manizales, Colombia, and M.Sc. (1999) and PhD (2008) in Electrical Engineering from Universidad de Los Andes, Bogot, Colombia. He is currently an Associate Professor with the Department of Electrical Engineering at School of Engineering, Universidad de Los Andes, Colombia where is involved in teaching courses on power electronics, fundamentals of power systems, power quality, distribution, and industrial systems design. His research interests include power quality and transients in grounding systems.